Reprinted from **Applied Optics**, Vol. 22, page 1684, June 1, 1983

Scattering phase matrix comparison for randomly hexagonal cylinders and spheroids

K. N. Liou, Q. Cai, P. W. Barber, and S. C. Hill

Scattering phase matrices are calculated for randomly oriented hexagonal cylinders and equivalent spheroids. The scattering solution for spheroids utilizes a numerical integral equation technique called the T-matrix method, while that for hexagonal cylinders employs a geometric ray-tracing method. Computational results show that there is general agreement for the phase functions P_{11} for hexagonal cylinders and spheroids with the same overall dimensions or surface area, except for the 22 and 46° halo features and the backscattering maximum produced by the hexagonal geometry. Values of P_{12} which are associated with linear polarization when the incident light is unpolarized differ in the forward directions where hexagonal cylinders have two positive polarization maxima. Large differences are observed in the P_{33} and P_{44} elements.

I. Introduction

Recent advances in electromagnetic scattering theory now make it possible to calculate exact scattering phase matrix elements for certain electrically large 3-D nonspherical objects. Asano and Sato,[1] for example, reported comprehensive single-scattering and polarization results for randomly oriented, identical spheroidal particles utilizing the solution of the wave equation in spheroidal coordinates. Most other techniques are based on integral equation formulations. One such approach is the T-matrix method, a numerical technique which has been applied to rotationally symmetric objects.[2] This method has been successfully used to determine the scattering, absorption, and polarization characteristics of dielectric spheroids and finite cylinders by Barber and Yeh[3] and Barber.[4] Utilizing another integral equation approach, Senior and Weil[5] developed a numerical technique to compute the scattering characteristics of hollow columnar ice crystals having size parameters <5. However, a general integral equation solution of scattering by hexagonal cylinders has not been available.

In a recent paper, Cai and Liou[6] developed a theory for the scattering of polarized light by hexagonal ice crystals utilizing the geometric ray-tracing technique. The six independent scattering phase matrix elements for randomly oriented large columns and small plates were calculated. It has been generally recognized that angular scattering and polarization behaviors of atmospheric ice crystals are fundamental to the development of remote-sensing techniques and to the understanding of radiative properties of cirrus. Since the above-mentioned T-matrix method is an exact solution to particles with spheroidal geometry, it appears of physical significance to understand the similarities and differences of the scattering phase matrix elements produced by this method and the hexagonal ray-tracing program. This will allow us to study whether the Mie type solution may be applicable to scattering and polarization computations involving ice crystals. In this brief paper we compare the calculated scattering phase matrix elements for randomly oriented ice crystals from the T-matrix method[3,4] using a spheroidal geometry and from the geometric optics method[6] using the hexagonal cylinder geometry. Since the T-matrix method is most efficient for smaller size parameters and the geometric optics method is only applicable for larger size parameters, we have selected size parameters of ~25 in major axes for columnlike and platelike crystals for comparison calculations. This size parameter is large enough for the geometric optics method to give reasonably accurate results, while small enough to give numerical T-matrix results without excessive computational efforts.

II. Comparison Results and Discussions

The basic geometrical parameters for hexagonal cylinders and spheroids selected for numerical computations are given in Table I. Two types of prolate and oblate spheroid are chosen for comparison purposes. The first case involves prolate and oblate spheroids with the same overall dimensions as the hexagonal column and plate, respectively. In the second case, the spheroids have the same surface area as the respective hexagonal cylinders. These values are shown in the table where the volumes are also listed for reference. Note that the volumes of the two spheroid cases bracket those of the corresponding hexagonal cylinders. The incident wavelength used is 0.7 μm, with the associated refractive index for ice of 1.31.

Scattering calculations were made for randomly ori-

P. W. Barber is with Clarkson College of Technology, Electrical and Computer Engineering Department, Potsdam, New York 13676; the other authors are with University of Utah, Salt Lake City, Utah 84112.

Received 9 November 1982.
0003-6935/83/111684-04$01.00/0.

Table I. Basic Geometrical Parameters for Hexagonal Cylinders and Spheroids

	Hexagonal column	Prolate spheroid 1	Prolate spheroid 2
Diameter (μm) $\times$ length (μm)	2×5	2×5	2.32×5.8
Surface area (μm^2)	35.2	26.15	35.2
Volume (μm^3)	13	10.45	16.4
	Hexagonal plate	Oblate spheroid 1	Oblate spheroid 2
Diameter (μm) $\times$ length (μm)	5×2	5×2	5.6×2.24
Surface area (μm^2)	62.48	50.0	62.48
Volume (μm^3)	32.5	26.2	36.55

ented hexagonal cylinders and spheroids in 3-D space. Random orientation of nonspherical particles with uniform sizes in 3-D space is generated by properly taking into account all possible orientation angles of the particles with respect to the incident beam (see, e.g., Cai and Liou,[6] Fig. 5) in zenith and azimuthal directions.

For nonspherical particles having a plane of symmetry and randomly oriented in 3-D space, the scattering phase matrix corresponding to the Stokes parameters (I,Q,U,V) contains only six independent elements in the form

$$\mathbf{P}(\theta) = \begin{bmatrix} P_{11} & P_{12} & 0 & 0 \\ P_{12} & P_{22} & 0 & 0 \\ 0 & 0 & P_{33} & -P_{43} \\ 0 & 0 & P_{43} & P_{44} \end{bmatrix}, \tag{1}$$

where the matrix is normalized so that the P_{11} element takes the form of the phase function, which satisfies the condition

$$\int_{4\pi} P_{11}(\Omega) d\Omega / 4\pi = 1. \tag{2}$$

In Fig. 1 comparisons are made of the normalized phase function P_{11} for the hexagonal columns and two types of prolate spheroid randomly oriented in space. For hexagonal columns the scattering pattern shows a strong peak located at ~22° scattering angle and a less strong feature at ~46° scattering angle. Both of these maxima are known as the halos produced by light rays undergoing two refractions through prime angles of 60 and 90°, respectively. There is also a broad maximum at ~160° scattering angle which is produced by internal reflections. In addition, the backscattering peak caused by internal reflections is rather pronounced. None of these features is shown in the scattering pattern for spheroids. However, there is a general agreement between the scattering patterns for hexagons and spheroids in the scattering angle from ~10 to 140°. Since the second spheroid case has a larger surface area than the first case, the diffraction peak is stronger in the former. However, compared with the hexagonal column, the diffraction peak for the spheroids is an order of magnitude smaller. Because the diameter-to-length ratio of the hexagonal column used is only 1/2.5, the diffraction peak is contributed from the light rays undergoing not only diffraction but also two refractions and external reflections. Thus, to make a proper comparison we have calculated the diffraction component only, and the result is depicted in the same diagram with a cross. The diffraction value is now very close to that of spheroid cases. From the optical principle, forward diffraction patterns depend on the geometric cross section of the particle. Since the cross sections of the randomly oriented hexagonal columns and the second prolate spheroid are identical, the forward diffraction patterns should be the same. The minor difference is probably attributable to the geometric optics approximation used in the hexagonal cylinder case.

Figure 2 compares the P_{12}, P_{22}, and P_{43} phase matrix elements. All elements are normalized with respect to P_{11}. The $-P_{12}/P_{11}$ element represents the degree of linear polarization for incident unpolarized light. In the hexagonal case, negative polarization is shown at the 22 and 46° halo maxima and at the backscattering angles. The largest positive polarization is found at a scattering angle of ~120°. For the two prolate spheroid cases negative polarization is seen from 30 to 60° scattering angles, while positve polarization is shown for all other angles. In sum, differences of the linear polarization patterns between hexagonal columns and prolate spheroids are in the forward and backscattering directions, where the sign of polarization reverses, except at the 22 and 46° halo angles. The P_{22}/P_{11} element is a measure of depolarization when the incident light is linearly polarized. For this element there is an agreement between hexagonal columns and prolate spheroids in the scattering angle range from 0 to ~70°, beyond which significant variations occur. Similarly for the P_{43}/P_{11} element we see a general resemblance between hexagons and spheroids in all scattering angles except in the area between 110 and 150°. For the spheroid cases, the effect of particle size on this element is also

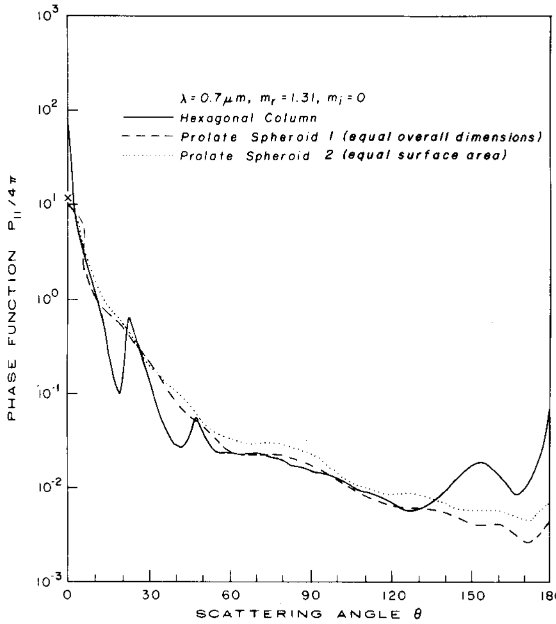

Fig. 1. Comparison of the normalized scattering phase function $P_{11}/4\pi$ for randomly oriented hexagonal ice columns and prolate spheroids as a function of the scattering angle. The prolate spheroid case in dots has the same surface area as the column. Cross at 0° scattering angle is obtained from diffraction only in the geometric optics program for hexagons.

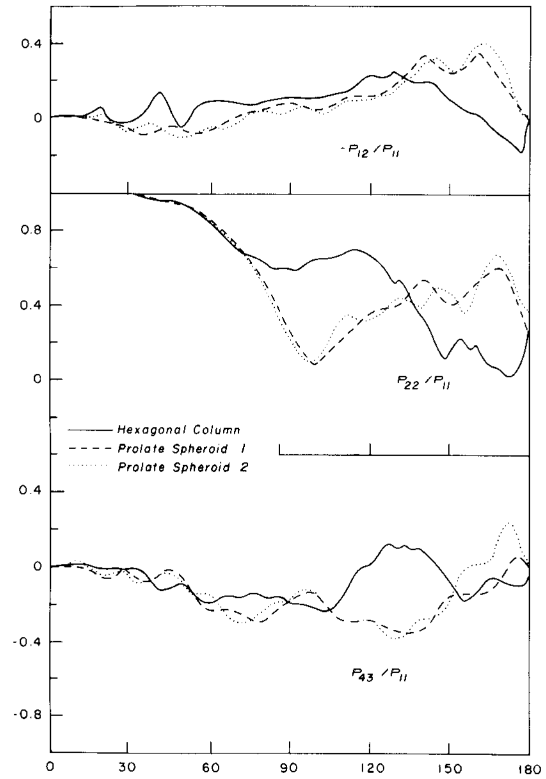

Fig. 2. Comparison of the phase matrix elements $-P_{12}/P_{11}$, P_{22}/P_{11}, and P_{43}/P_{11} for hexagonal ice columns and prolate spheroids as a function of the scattering angle.

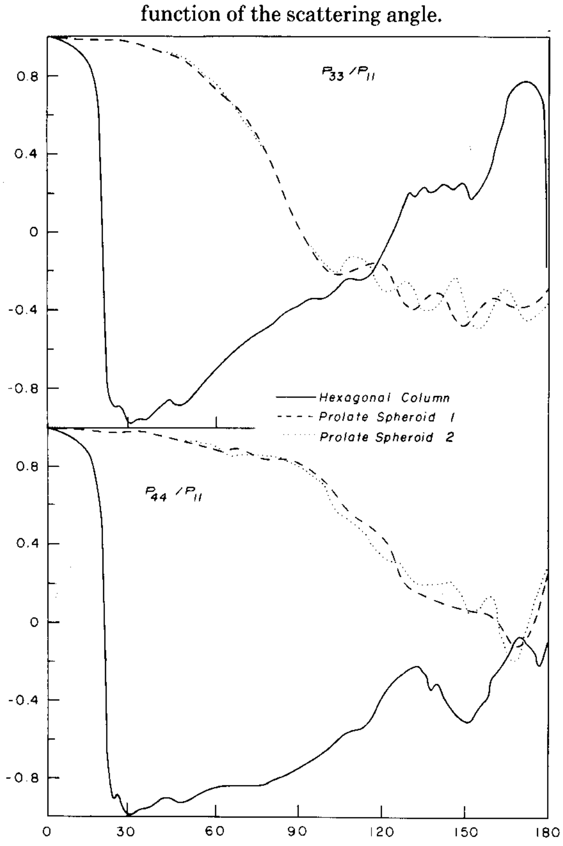

Fig. 3. Comparison of the phase matrix elements P_{33}/P_{11} and P_{44}/P_{11} for hexagonal ice columns and prolate spheroids as a function of the scattering angle.

seen in the backscattering angles. Generally speaking, deviations of these three elements for hexagonal columns from those for prolate spheroids are found in certain scattering angle ranges, where presumably the shape effect is the primary cause.

The P_{33}/P_{11} and P_{44}/P_{11} elements are shown in Fig. 3. These two elements are similar for the hexagonal columns but both elements deivate greatly from the prolate spheroid results. Basically, the largest differences occur at ~30° scattering angle, where the hexagonal case has a value of −1, whereas the spheroid case shows a value very close to +1. For the hexagonal case, P_{33}/P_{11} and P_{44}/P_{11} values decreased rapidly from −1 to +1 between the scattering angles 0–20°. Differences between the two spheroid cases result from their slightly different sizes.

Comparisons of the scattering phase matrix elements for hexagonal plates and oblate spheroids are shown in Figs. 4–6. For the P_{11} element shown in Fig. 4, hexagonal plates reveal a similar scattering pattern as that of columns, but the 22° halo feature and the broad maximum at ~150° scattering angle are reduced somewhat. Results for oblate spheroids show a number of maxima and minima because they have larger surface areas as well as volume (see Table I) than those of prolate spheroids. Comparisons of the backscattering values in the oblate spheroid and hexagonal plate cases are better than their counterparts in the prolate spheroid and hexagonal column cases. Also note that the diffraction peak in the oblate case is slightly greater than that in the prolate case because of the larger cross-sectional area. We have also run geometric optics calculations in the plate case without adding the contribution due to two refractions and external reflections, and the diffraction peak result is denoted by a cross in this diagram. This value is very close to but not exactly the same as the diffraction peak produced in the oblate spheroid case 2.

In Fig. 5 we see that the P_{12}/P_{11}, P_{22}/P_{11}, and P_{43}/P_{11} elements for the hexagonal plates and oblate spheroids compare well in all scattering angles, although there are variations in detailed features. The linear polarization pattern $-P_{12}/P_{11}$ for oblate spheroids now shows negative values in scattering angles from ~160 to 180°, while the plates generate larger negative polarization in this region than the columns. We also find that the position of the maximum polarization in the plate case shifts to a smaller scattering angle compared with that in the column case, and the magnitude of the maximum polarization is now reduced to ~20%. Linear polarization patterns for oblate and prolate spheroids show some differences which are basically the result of size and shape effects. Patterns of the element P_{22}/P_{11} for hexagonal plates and oblate spheroids are in general agreement. While there are variations in the element P_{43}/P_{11}, agreements between the plate and oblate spheroids are also good. Results of P_{33}/P_{11} and P_{44}/P_{11} again show large differences between the hexagonal column and spheroid cases. The hexagonal plate result has an interesting small peak at ~20° scattering angle which is not seen in the column case.

III. Summary

We have carried out a comparison program between the scattering phase matrix elements for randomly oriented hexagonal cylinders and spheroids using a geometric ray-tracing program and a numerical integral equation approach, respectively. For the scattering phase function P_{11}, results for hexagonal columns and prolate spheroids and for hexagonal plates and oblate spheroids are generally comparable, except that the 22 and 46° halo features and backscattering maximum produced by the hexagonal geometry do not exist in the spheroid cases. Values of the linear polarization ($-P_{12}/P_{11}$) differ in the forward directions, where hexagonal cylinders have two positive polarization maxima associated with negative polarization minima of the halos. There is a general agreement between the elements P_{22}/P_{11} and P_{43}/P_{11} for hexagonal cylinders and spheroids with the same overall dimensions or surface area. Results also revealed that plates and oblate spheroids compare better than the columns and prolate spheroids. Large differences are found in the elements P_{33}/P_{11} and P_{44}/P_{11} for all cases.

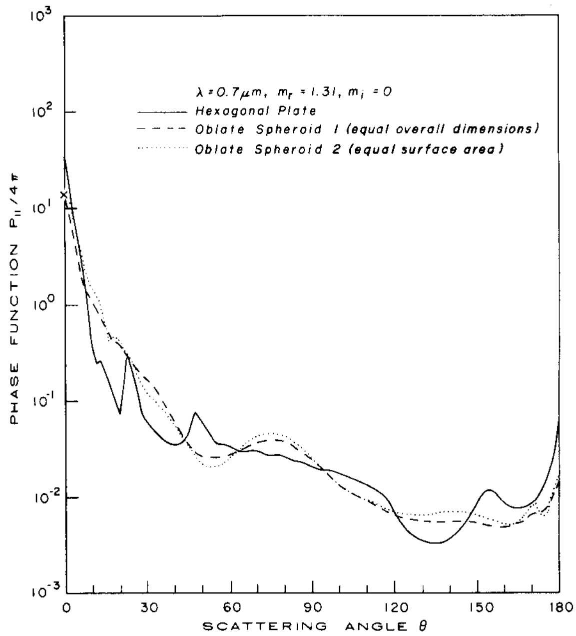

Fig. 4. Same as Fig. 1, except for hexagonal plates and oblate spheroids.

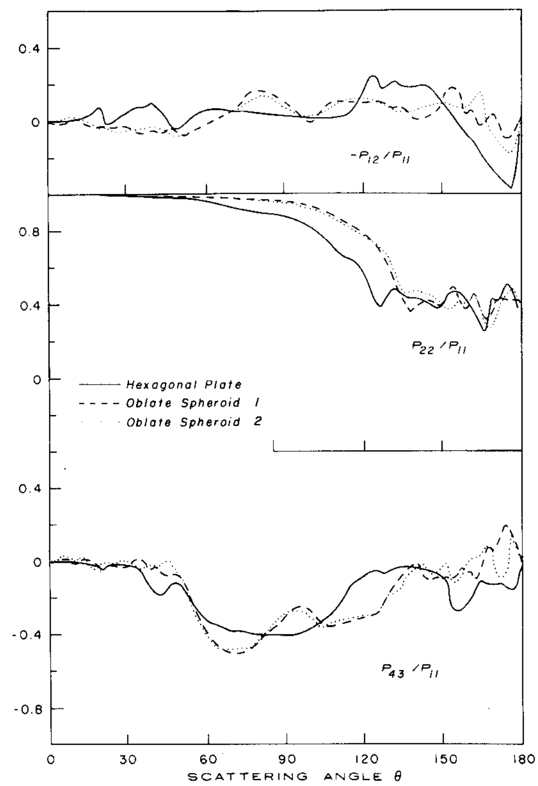

Fig. 5. Same as Fig. 2, except for hexagonal plates and oblate spheroids.

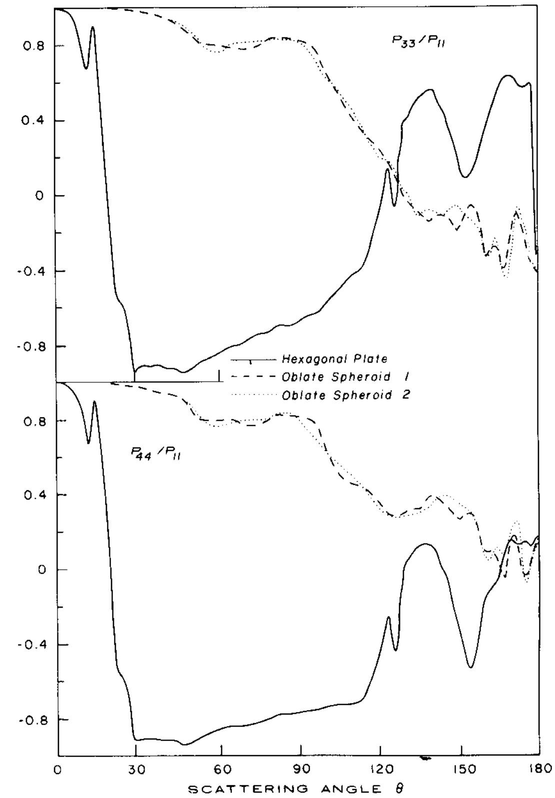

Fig. 6. Same as Fig. 3, except for hexagonal plates and oblate spheroids.

This research was supported by the Division of Atmospheric Sciences of the National Science Foundation under grant ATM-81-09050, the Air Force Office of Scientific Research under contract F49620-79-C-0198, and by the U.S. Army Research Office. We thank Sharon Bennett for typing and editing the manuscript.

References

1. S. Asano and M. Sato, Appl. Opt. **19**, 962 (1980).
2. P. C. Waterman, Phys. Rev. D **3**, 825 (1971).
3. P. W. Barber and C. Yeh, Appl. Opt. **14**, 2864 (1975).
4. P. W. Barber, IEEE Trans. Microwave Theory Tech. **MTT-25**, 373 (1977).
5. T. B. A. Senior and H. Weil, Appl. Opt. **16**, 2979 (1977).
6. Q. Cai and K. N. Liou, Appl. Opt. **21**, 3569 (1982).